

# DIVA: A Dirichlet Process Based Incremental Deep Clustering Algorithm via Variational Auto-Encoder

**Zhenshan Bing \***

Technical University of Munich  
zhenshan.bing@tum.de

**Yuan Meng \***

Technical University of Munich  
y.meng@tum.de

**Yuqi Yun \***

Technical University of Munich  
yuqi.yun@tum.de

**Hang Su**

Politecnico di Milano  
hang.su@polimi.it

**Xiaojie Su**

Chongqing University  
suxiaojie@cqu.edu.cn

**Kai Huang**

Sun Yat-sen University  
huangk36@mail.sysu.edu.cn

**Alois Knoll**

Technical University of Munich  
knoll@in.tum.de

## Abstract

Generative model-based deep clustering frameworks excel in classifying complex data, but are limited in handling dynamic and complex features because they require prior knowledge of the number of clusters. In this paper, we propose a nonparametric deep clustering framework that employs an infinite mixture of Gaussians as a prior. Our framework utilizes a memoized online variational inference method that enables the “birth” and “merge” moves of clusters, allowing our framework to cluster data in a “dynamic-adaptive” manner, without requiring prior knowledge of the number of features. We name the framework as **DIVA**, a **D**irichlet Process-based **I**ncremental deep clustering framework via **V**ariational **A**uto-**E**ncoder. Our framework, which outperforms state-of-the-art baselines, exhibits superior performance in classifying complex data with dynamically changing features, particularly in the case of incremental features.

## 1 Introduction

Clustering is a key task in unsupervised learning that aims to group data points based on similarity or dissimilarity metrics. Recently, deep clustering algorithms that combine deep neural networks with clustering methods have shown great promise in various applications, such as image segmentation [1, 2], document clustering [3, 4], and anomaly detection [5].

Generative model-based deep clustering algorithms have emerged as a promising research direction, with the variational auto-encoder (VAE) [6] being a popular choice due to its ability to learn data representations and generation [2]. VAE-based clustering methods typically involve two stages: training a VAE to learn the underlying data distribution and then using the learned latent variables for clustering. The advantage of VAE is its ability to handle non-linear and complex distributions [1].

A natural idea in this field is to combine the Gaussian mixture model (GMM) [7], which is a highly representative clustering module, with the VAE framework. This framework employs GMM as prior to provide with a richer information capacity, while the VAE’s powerful representation learning and reconstruction capabilities can overcome the negative impact of the GMM shallow structure

\* Authors contribute equally.

on the weak representation of non-linearity [1]. However, such frameworks still have limitations, including the need to specify the number of clusters beforehand, which can be challenging when the number is unknown or varies across datasets. In Bayesian nonparametric field, previous work tried to replace the parameters of the isotropic Gaussian prior of standard VAE with the stick-breaking proportions of a Dirichlet process [8]. Unfortunately, in this case the shape and density of individual component cannot be well defined. To address this issue, we propose using the Dirichlet process mixture model (DPMM) [9] from nonparametric Bayes as a clustering module for our framework. DPMM’s random probability measure sampled from the base distribution through the stick-breaking process maintains both discrete and continuous characteristics, and the number of components can theoretically reach infinity, overcoming the problem of pre-specifying the number of components. Additionally, we use the “birth” and “merge” behavior provided by DPMM for dynamic feature adaptation, allowing our framework to dynamically adjust the number of components according to the observed data to improve clustering performance. Our proposed framework demonstrates superior clustering performance and disentangled representation learning ability in various datasets, specially in facing incremental features, where the number of features in datasets gradually increases during training. This study presents novel insights on incorporating DPMM as a prior for the VAE and utilizing the “birth” and “merge” behavior to dynamically adjust the number of clusters in generative deep clustering framework.

The contributions of our paper are summarized as follows: First, we eliminate pre-defining the cluster number in prior space by introducing nonparametric clustering module DPMM into our VAE-based framework, allowing for clustering data with infinite features. Second, we introduce a memoized online variational Bayes inference method into the framework, which enables dynamic changes in the number, density, and shape of clusters in the prior space according to the observations. This allows for “birth” and “merge” of clusters. Third, we verify the dynamic-adaptation ability of our proposed framework, DIVA, demonstrating its effectiveness against state-of-the-art baselines in facing incremental data features. We show that DIVA can dynamically adjust the clusters in the feature-increasing dataset to maintain a high level of unsupervised clustering accuracy. The dynamic adaptation capability of DIVA demonstrated in our study has the potential to inspire new approaches to tackling the challenge of catastrophic forgetting [10], and could be extended to domains such as continuous learning [11] and meta-reinforcement learning [12–14].

## 2 Related work

Clustering is a fundamental task in machine learning, with widely used models such as  $k$ -means [15] or Gaussian mixture models [7] from Bayes parametrics. Bayesian non-parametric methods provide a flexible framework to handle an unknown number of clusters, with representative models like Dirichlet process mixture model [16], Chinese Restaurant Process (CRP) [17], Pitman-Yor Process (PYP) [18], and Hierarchical Dirichlet Process (HDP) [19] commonly used in clustering. However, these models have limitations in handling complex data distributions due to their shallow structure. To address this, deep neural network-based clustering algorithms have been proposed. DEC [20] uses a  $k$ -means model with a Student’s  $t$ -distribution kernel to estimate the similarity between feature embeddings and cluster centroids. DeepCluster [21] employs a similar approach, iteratively updating the cluster assignments using a  $k$ -means model. SCAN [22] uses a fine-tuning and pre-trained framework, fine-tuning the clustering results with self-labeling. In addition, generative model-based deep clustering algorithms have gained popularity due to their powerful representation learning ability. VaDE [23] employs a VAE to learn a low-dimensional embedding space and a mixture of Gaussians to model the cluster assignment. GMVAE [24], an extension of VaDE, models the data distribution with a more flexible GMM. Stick-breaking VAE [8] leverages stick-breaking as its prior distribution, allowing for infinite mixtures. Last but not least, Generative Adversarial Networks (GANs) have also been applied to clustering problems, examples include Mixture of GANs [25], DCGAN [26] and its extension [27], and MIC-GANs [28]. We refer to [1, 2] for complete literature surveys about generative model based deep clustering algorithms.

## 3 Preliminaries

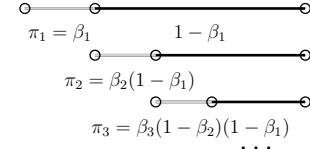
In this section, we introduce the concept of Bayesian nonparametric models and then the variational inference methods, which provide the theoretical foundation of our framework.

### 3.1 Dirichlet process and stick-breaking method

The Dirichlet process (DP) is a distribution over probability measures [29], where the marginal distribution is Dirichlet-distributed, resulting in random distributions. Given a base distribution  $H$  and a positive concentration parameter  $\alpha$ , a random probability measure  $G$  is DP-distributed, denoted as  $G \sim \text{DP}(\alpha, H)$ . For a detail explanation of DP's properties, please refer to [9, 29].

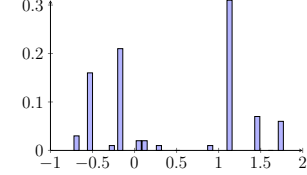
A DP can be defined constructively using the Stick-Breaking (SB) process [16] via Beta distribution  $\mathcal{B}$ , where for  $k \geq 1$ :  $\beta_k \sim \mathcal{B}(1, \alpha)$ ,  $\pi_k = \beta_k \prod_{i=1}^{k-1} (1 - \beta_i)$ . In this process, a unit-length stick is imaginatively broken into an infinite number of segments  $\pi_k$ , with  $\alpha$  being a positive scalar. We first sample  $\beta_1 \sim \mathcal{B}(1, \alpha)$  from a Beta distribution and break the stick with length  $\pi_1 = \beta_1$ . We then sample  $\beta_2$ , and the length of the second segment will be  $\pi_2 = \beta_2(1 - \beta_1)$ . Continuing this process, we have  $\sum_{k=1}^{\infty} \pi_k = 1$ , and the resulting  $\pi$  follows a Griffiths-Engen-McCloskey (GEM) distribution  $\pi \sim \text{GEM}(\alpha)$ . Figure 1a shows an intuitive image about the SB process.

Since a random distribution  $G$  drawn from a DP maintains discrete property, it can be expressed as a weighted sum of point masses, namely  $G = \sum_{k=1}^{\infty} \pi_k \delta_{\theta_k^*}$  [30], where  $\delta_{\theta_k^*}$  is the point mass located at  $\theta_k^*$ : it equals 1 at  $\theta_k^*$  and equals 0 elsewhere. By sampling the weights  $\pi_k$  according to SB-process and sampling  $\theta_k$  from a base distribution  $\theta_k \sim H$ , we can say that  $G \sim \text{DP}(\alpha, H)$ , indicating that  $G$  is a Dirichlet Process with the base distribution  $H$  and concentration parameter  $\alpha$ . Figure 1b shows a draw from a DP with  $\alpha = 5$ .



(a) Stick-breaking process.

$H = \mathcal{N}(0, 1), \alpha = 5$



(b) Draw of a DP.

Figure 1: (a) Stick-breaking process. (b) Histogram of  $\text{DP}(\alpha = 5, H = \mathcal{N}(0, 1))$ .

### 3.2 Dirichlet process mixture model

DP mixture is a representative generative Bayesian nonparametric model that uses an infinite mixture of clusters to model a set of observations  $\mathbf{x} = x_{1:N}$ , where the number of cluster components is not predefined but rather determined by the observations.

The model assumes that each data point  $x_i$  is sampled from a distribution  $F(\theta_i)$  parameterized by a latent variable  $\theta_i$  drawn independently from a probability measure  $G$ . The DPMM assumes a DP prior  $G|\alpha, H \sim \text{DP}(\alpha, H)$ , which introduces discreteness and clustering property where  $\theta_i$  takes on repeated values. Then all  $x_i$ 's drawn with the same value of  $\theta_i$  can be seen as one cluster, resulting in the clustering of observations. The number of unique values of  $\theta_i$  determines the active number of cluster components, which can be dynamically inferred during inference from the observed data. Let  $v_i$  be a cluster assignment variable that takes on value  $k$  with probability  $\pi_k$  drawn from a categorical distribution (Cat). The DPMM can be expressed via the stick-breaking process, where the mixing proportions  $\pi$  are sampled from a GEM distribution and the prior  $H$  over the cluster parameters is the base distribution of an underlying DP measure  $G$ . Specifically, we have:

$$\theta_k^* | H \sim H, \quad \pi | \alpha \sim \text{GEM}(\alpha), \quad v_i | \pi \sim \text{Cat}(\pi), \quad x_i | v_i \sim F(\theta_{v_i}^*), \quad (1)$$

where  $\theta_k^*$  are the cluster parameters,  $\pi$  is the mixing proportion,  $F(\theta_{v_i}^*)$  is the distribution over observation in cluster  $k$ , and  $H$  is the prior over cluster parameters. Typically,  $F$  is a Gaussian distribution. To provide an intuitive understanding, we draw the generative graphic model for DPMM in Figure 2.

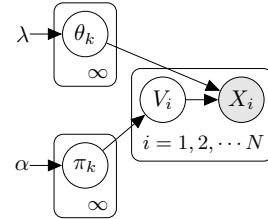


Figure 2: Generative graphic model of DPMM

### 3.3 Variational inference for DPMM

In this section, we introduce variational inference as a method for approximating the posterior density for models based on observed data, with a focus on Bayesian nonparametric models.

The basic idea of variational inference is to convert the inference problem into an optimization problem. Refer from (1), we write the joint probability for DPMM as

$$p(\mathbf{x}, \mathbf{v}, \boldsymbol{\theta}, \boldsymbol{\beta}) = \prod_{n=1}^N F(x_n | \theta_{v_n}) \text{Cat}(v_n | \boldsymbol{\pi}(\boldsymbol{\beta})) \prod_{k=1}^{\infty} \mathcal{B}(\beta_k | 1, \alpha) H(\theta_k | \lambda) \quad (2)$$

Since the true posterior  $p(\mathbf{v}, \boldsymbol{\theta}, \boldsymbol{\beta} | \mathbf{x})$  is intractable, we aim to find the best variational distribution  $q(\mathbf{v}, \boldsymbol{\theta}, \boldsymbol{\beta})$  that minimizes the KL divergence with the exact conditional:

$$q^*(\mathbf{v}, \boldsymbol{\theta}, \boldsymbol{\beta}) = \arg \min_q \mathbb{KL}(q(\mathbf{v}, \boldsymbol{\theta}, \boldsymbol{\beta}) || p(\mathbf{v}, \boldsymbol{\theta}, \boldsymbol{\beta} | \mathbf{x})) \quad (3)$$

$$\mathbb{KL}(q(\mathbf{v}, \boldsymbol{\theta}, \boldsymbol{\beta}) || p(\mathbf{v}, \boldsymbol{\theta}, \boldsymbol{\beta} | \mathbf{x})) = \mathbb{E}[\log q(\mathbf{v}, \boldsymbol{\theta}, \boldsymbol{\beta})] - \mathbb{E}[\log p(\mathbf{x}, \mathbf{v}, \boldsymbol{\theta}, \boldsymbol{\beta})] + \log p(\mathbf{x})$$

Notice that  $\log p(\mathbf{x})$  does not depend on  $q$ , so instead of minimizing the KL divergence directly, we maximize the evidence lower bound (ELBO), which consists of the expected log-likelihood of the data  $\mathbb{E}[\log p(\mathbf{x} | \mathbf{v}, \boldsymbol{\theta}, \boldsymbol{\beta})]$  and the KL divergence between two priors  $\mathbb{KL}(q(\mathbf{v}, \boldsymbol{\theta}, \boldsymbol{\beta}) || p(\mathbf{v}, \boldsymbol{\theta}, \boldsymbol{\beta}))$ , according to the eq. (3), the ELBO can be rewritten as:

$$\begin{aligned} \text{ELBO}(q) &= \mathbb{E}[\log p(\mathbf{x}, \mathbf{v}, \boldsymbol{\theta}, \boldsymbol{\beta})] - \mathbb{E}[\log q(\mathbf{v}, \boldsymbol{\theta}, \boldsymbol{\beta})] \\ &= \mathbb{E}[\log p(\mathbf{x} | \mathbf{v}, \boldsymbol{\theta}, \boldsymbol{\beta})] - \mathbb{KL}(q(\mathbf{v}, \boldsymbol{\theta}, \boldsymbol{\beta}) || p(\mathbf{v}, \boldsymbol{\theta}, \boldsymbol{\beta})) \end{aligned} \quad (4)$$

Therefore, the optimization of the ELBO is interpreted as finding a solution that explains the observed data with minimal deviation from the prior.

For the DPMM model, based on the idea of variational inference, we define the variational distribution  $q$  following the mean-field assumption, where each latent variable has its variational factor and is mutually independent of each other, namely  $q(\mathbf{v}, \boldsymbol{\theta}, \boldsymbol{\beta}) = \prod_{n=1}^N q_{v_n} \prod_{k=1}^K q_{\beta_k} q_{\theta_k}$ , where  $q_{v_n} = \text{Cat}(v_n | \hat{r}_{n1:n_K})$ ,  $q_{\beta_k} = \mathcal{B}(\beta_k | \hat{\alpha}_{k1}, \hat{\alpha}_{k0})$ ,  $q_{\theta_k} = H(\theta_k | \hat{\lambda}_k)$ . In the context of variational inference, the true posterior distribution is infinite, and only an approximate distribution can be obtained. However, as the number of components  $K$  in categorical factor increases, the optimized ELBO objective can result in a variational distribution that closely approximates the infinite posterior. Thus to enable computation, we limit the categorical factor to only finite  $K$  components, in which  $K$  is large enough to cover all potential features. We also consider a special case where the distributions  $H$  and  $F$  come from the exponential family. Hughes and Sudderth [9] showed that in this case, the ELBO is expressed in terms of the expected mass  $N_k$  and the expected sufficient statistic  $s_k(x)$  of each component  $k$ :

$$\begin{aligned} \text{ELBO}(q) &= \sum_{k=1}^K \left[ \mathbb{E}_q[\theta_k]^T s_k(x) - \hat{N}_k[a(\theta_k)] + \hat{N}_k[\log \pi_k(\beta)] - \sum_{n=1}^N \hat{r}_{nk} \log \hat{r}_{nk} \right. \\ &\quad \left. + \mathbb{E}_q \left[ \log \frac{\mathcal{B}(\beta_k | 1, \alpha)}{q(\beta_k | \hat{\alpha}_{k1}, \hat{\alpha}_{k0})} \right] + \mathbb{E}_q \left[ \log \frac{H(\theta_k | \lambda)}{q(\theta_k | \hat{\lambda}_k)} \right] \right], \end{aligned} \quad (5)$$

Then each variational factor can be updated individually in an iterative manner. In first stage, we update the *local* variational parameters  $\hat{r}_{nk}$  in the categorical factor  $q_{v_n}$  for each cluster assignment. In second stage, we update the *global* parameters  $\hat{\alpha}_{k1}$ ,  $\hat{\alpha}_{k0}$ ,  $\hat{\lambda}_k$  in the factors for stick-breaking proportion  $q_{\beta_k}$  and the factors for base distribution  $q_{\theta_k}$  [31]. For the detail derivation and implementation please refer to our appendix Sec. A.1.

The computation of the summary statistics  $N_k$  and  $s_k(x)$  requires the full dataset. For inference on a large dataset, we use a batch-based approach called memoized online variational Bayes (memoVB) [9], which breaks the summary statistics of full data into a sum of the summary statistics of each batch. The DPMM has nonparametric nature, which means it can adjust to varying numbers of clusters. This property enables the development of heuristics for dynamically adding or removing clusters, which can help avoid local optima when using batch-based variational inference approaches.

MemoVB is an approach that implements birth and merge moves for dynamic cluster adjustment. To create new clusters, we collect poorly described subsamples  $x'$  by a single cluster when passing through each batch and fit a separate DPMM model with  $K'$  initial clusters. Assuming that the active number of clusters before the birth move is  $K$ , we can either accept or reject the new cluster proposals by comparing the result of assigning  $x'$  to  $K + K'$  with that of assigning  $x'$  to  $K$ . To complement the birth move, a merge move potentially combines a pair of clusters into one. Two clusters are merged if the merge improves the ELBO objective, leaving  $K - 1$  clusters after the merge ELBO [9].

## 4 Methodology

In this section, we present DIVA, a novel deep clustering approach that integrates a Bayesian nonparametric model with a variational autoencoder.

Given an unlabeled set of data with  $n$  points  $\{x_i\}_{i=1}^n \in X$ , the designed deep clustering method that simultaneously learns: (1) The latent representation  $z_i$  of each  $x_i$  in a  $D$ -dimensional Gaussian latent space  $Z$  and the mapping  $f_\theta : X \rightarrow Z$  that projects the data points  $\{x_i\}_{i=1}^n \in X$  onto the latent space  $Z$ . (2) The number  $K$  of Gaussian-distributed clusters and their associated means  $\mu_k$  and covariance matrices  $\Sigma_k$ . (3) The cluster assignment  $v_i$  of each  $x_i$ , where  $v_i \in \{1, \dots, K\}$ . (4) The reconstructions  $x_i^*$  of the inputs via decoder network.

To accomplish this, DIVA combines a standard VAE with a DPMM, where the cluster assignments are jointly determined by the learned representation and the cluster distributions. Our algorithm uses an alternating optimization scheme: First, we update the DPMM module using the latent variables  $z_i$ , which are sampled from the encoder using the reparametrization trick during the last VAE update. Then the DPMM module is fixed, and the VAE parameters are updated, using the assigned clusters to each  $z_i$  to minimize the KL divergence. An overview of DIVA is shown in Figure 3.

### 4.1 Updating the DPMM

When updating the parameters of the DPMM, we fit a DPMM on the latent samples  $z_i$ 's obtained from the VAE. We define the generative process of assigning data points to clusters according to the SB process. A generative process is assumed as follows: (1) The mean  $\mu_k$  and diagonal covariance matrix  $\Sigma_k$  of each cluster  $k$  are drawn from a Normal-Wishart distribution, which is the conjugate prior for a diagonal Gaussian with unknown means and unknown covariance matrix, namely  $\Sigma_k \sim \mathcal{W}(\mathbf{W}, \nu)$ ,  $\mu_k \sim \mathcal{N}(\mu_0, (\lambda \Sigma_k)^{-1})$ , assuming the latent space is  $D$ -dimensional. (2) The probabilities of each cluster are drawn from a GEM distribution with concentration parameter  $\alpha$ ,  $\pi \sim \text{GEM}(\alpha)$ , as described in Sec. 3.1. (3) The cluster assignment  $v_n$  is drawn from a discrete distribution  $\text{Cat}(\pi)$  based on the cluster probabilities previously obtained, which is  $\pi \sim \text{GEM}(\alpha)$ . (4)

In our DPMM module, when the latent variable  $z_i$  is assigned to a cluster  $v_n = k$ , we assume that it is sampled from a multivariate Gaussian with mean  $\mu_k$  and variance  $\Sigma_k$ , which means  $z_i | v_n = k \sim \mathcal{N}(\mu_k, \Sigma_k)$ . (5) The original data are assumed to be generated by the decoder, namely  $f_\theta(z_i) = x_i$ , where  $\theta$  are the parameters of the decoder.

Given the overall generative process, the DPMM has a joint probability

$$p(\mathbf{z}, \mathbf{v}, \boldsymbol{\beta}, \boldsymbol{\mu}, \Sigma) = \prod_{i=1}^N \mathcal{N}(z_i | \mu_{v_n}, \Sigma_{v_n}) \text{Cat}(v_n | \boldsymbol{\pi}(\boldsymbol{\beta})) \prod_{k=1}^{\infty} \mathcal{B}(\beta_k | 1, \alpha) \prod_{k=1}^{\infty} \mathcal{N}(\mu_k | \mu_0, (\lambda \Sigma_k)^{-1}) \mathcal{W}(\Sigma_k | \mathbf{W}, \nu) \quad (6)$$

We then use variational inference to find the posterior estimates for the parameters. We construct the variational distribution  $q$  with the following factorization:

$$q(\mathbf{v}, \boldsymbol{\beta}, \boldsymbol{\mu}, \Sigma) = \prod_{n=1}^N \text{Cat}(v_n | \hat{r}_{n_1}, \dots, \hat{r}_{n_K}) \prod_{k=1}^K \mathcal{B}(\beta_k | \hat{\alpha}_{k_1}, \hat{\alpha}_{k_0}) \prod_{k=1}^K \mathcal{N}(\mu_k | \hat{\mu}_0, (\hat{\lambda} \Sigma_k)^{-1}) \mathcal{W}(\Sigma_k | \hat{\mathbf{W}}, \hat{\nu}). \quad (7)$$

We propose the iterative optimization procedure described in Sec. 3.3 that updates the Normal-Wishart distribution parameters  $\hat{\mu}_0$ ,  $\hat{\lambda}$ ,  $\hat{\mathbf{W}}$ , and  $\hat{\nu}$  in each step. We also utilize the memoized online variational Bayes method to update the parameters of the stick-breaking process  $\hat{r}_{n_1:n_k}$ ,  $\hat{\alpha}_{k_1}$ , and  $\hat{\alpha}_{k_0}$ .

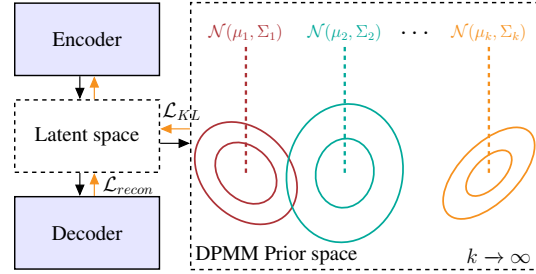


Figure 3: Overview of the DIVA. We optimize the DPMM and the VAE alternately. When updating the DPMM, we use the current latent sample  $z$  obtained from the VAE. When updating the VAE, we assign the outputs of the encoder to the clusters of the current DPMM and minimize the KL divergence with respect to the assigned cluster.

to estimate the cluster probabilities and assignments. In addition, we dynamically adjust the total number of clusters  $K$  using birth-and-merge moves. A complete update for our DPMM module thus breaks down to updating three sets of parameters.

Each update of the DPMM module is performed after a training epoch of the VAE. Since we alternate between updating the DPMM module and the VAE, the DPMM module is not required to converge in each update and avoids the need to fit a new DPMM model from scratch every time. In each update, we initialize the DPMM with the parameters learned from the previous updates and apply this module to new latent samples produced by the updated VAE, enabling us to update the same DPMM while incorporating the latest changes in the latent space mappings.

## 4.2 Updating the VAE

When training the VAE, we jointly minimize the reconstruction loss  $\mathcal{L}_{recon}$  and the KL divergence loss  $\mathcal{L}_{KL}$ . The reconstruction loss  $\mathcal{L}_{recon}$  is the mean squared error between the observed data  $x$  and the decoder’s reconstructions  $x^*$ , which is kept from standard VAE. The  $\mathcal{L}_{KL}$  is simply the KL-divergence between two isotropic Gaussian distributions [6].

To compute  $\mathcal{L}_{KL}$ , we obtain the cluster assignment  $v_i = k$  of each latent sample  $z_i$  from the current DPMM model. Using the DPMM, the mean and covariance matrix of assigned cluster  $k$  is  $\mu_k$  and  $\Sigma_k$ . According to VAE,  $z_{id} = \mu_d(x; \phi) + \sigma_d(x; \phi)\eta$  for  $d \in \{1, 2, \dots, D\}$ , where  $\phi$  are encoder parameters,  $\mu(x_i; \phi)$  and  $\sigma(x_i; \phi)$  are encoder outputs and  $\eta \sim \mathcal{N}(0, 1)$ . The KL divergence between two multivariate Gaussian distributions is calculated as follows:

$$D_{KL_{ik}} = \frac{1}{2} \left[ \log \frac{|\Sigma_k|}{|\Sigma(x_i; \phi)|} - D + \text{tr}\{\Sigma_k^{-1} \Sigma(x_i; \phi)\} + (\mu_k - \mu(x_i; \phi))^T \Sigma_k^{-1} (\mu_k - \mu(x_i; \phi)) \right] \quad (8)$$

However, this hard assignment method may assign a sample to a wrong cluster, introducing errors into the training by calculating the KL divergence. To overcome this issue, we introduce *soft assignment*, in which we compute the probability  $p_{ik}$  of assigning the latent sample  $z_i$  to cluster  $k$  using the DPMM for all possible  $k \in \{1, 2, \dots, K\}$ . Then the KL divergence is defined as a weighted sum with respect to each cluster:

$$D_{KL_i} = \sum_{k=1}^K p_{ik} D_{KL_{ik}} \quad (9)$$

Although one can use a more complex weighting strategy, we found this simple weighting by probabilities to be sufficient empirically. We use Algorithm 1 to summarize the DIVA algorithm.

---

### Algorithm 1 DIVA

---

**Require:** Dataset  $\mathcal{D}$ , batch size  $B$ , DPMM train steps  $T$ , parameters  $\phi$  of the encoder and  $\theta$  of the decoder.

- 1: Initialize  $\phi$ ,  $\theta$  of VAE, the DPMM with  $K = 1$ , including  $\mu_0, \lambda, \mathcal{W}, \nu$  and  $\alpha$ .
- 2: **repeat**
- 3:   Sample mini-batch  $\mathcal{M} = \{x_{0:B}\} \sim \mathcal{D}$ .
- 4:   With the VAE, obtain latent variables  $z_{0:B}$  and save to a buffer  $\mathcal{Z} = \mathcal{Z} \cup \{z_{0:B}\}$ .
- 5:   With the current DPMM, obtain the cluster assignments  $v_{0:B}$  and the assignment probabilities of each latent variable.
- 6:   Compute  $\mathcal{L}_{KL}$  using (8), (9),  $\mathcal{L}_{recon}$  and update  $\phi, \theta$ .
- 7:   **if** time to update the DPMM (e.g. at the end of an epoch) **then**
- 8:     **for** step  $i = 1, 2, \dots, T$  **do**
- 9:       Update DPMM variables  $\hat{\mu}_0, \hat{\lambda}, \hat{\mathcal{W}}, \hat{\nu}, \hat{r}_{n_1:n_k}, \hat{\alpha}_{k_1}, \hat{\alpha}_{k_0}$  using  $\mathcal{Z}$  and current DPMM.
- 10:       birth moves to try to add new clusters, and merge moves to try to combine existing clusters.
- 11:     Reset buffer  $\mathcal{Z} = \emptyset$ .
- 12: **until** convergence.

---

## 5 Experiments

In this section, we verify the dynamic-adaptive clustering ability of DIVA and show its effectiveness in clustering when facing dynamically increased data features.

## 5.1 Implementation details

We select three recognized representative, widely adopted datasets for verification, including two image datasets MNIST [32], Fashion-MNIST [33] and a text classification dataset Reuters10k [23], where we normalize images on MNIST and Fashion-MNIST. Using Reuters10k can evaluate the generalization ability of our model beyond bare image classification tasks.

We compared our proposed method to three baselines: GMM [7], GMVAE [24], and SB-VAE [8]. GMM is a representative clustering module in the Bayes parametrics. GMVAE builds upon GMM by incorporating it as a prior and jointly learning the representation and clustering. SB-VAE replaces the isotropic Gaussian with a Stick-breaking distribution, which offers infinite clustering capability. Both GMVAE and SB-VAE are state-of-the-art algorithms in Bayes parametric and non-parametric generative deep clustering. Since the number of clusters in the prior space must be pre-defined in GMM and GMVAE, we thus select the cluster number  $K = 3, 5, 10$  for both baselines. For image datasets, We use a 2-layer convolutional networks for our VAE encoder, the latent dimension is 16. For text dataset, we use 3 full-connection layers as our VAE architecture, the latent space has 100 dimension. For more details please refer to the appendix Sec. A.2.

In order to evaluate the unsupervised clustering performance of our framework on various datasets, here we leverage the metrics about the unsupervised clustering accuracy and kNN error from previous works [20, 23] as our key metrics. For both image datasets we run for all frameworks 100 epochs and evaluate the performance on the test dataset. For Reuters10k, we train for all frameworks 15 epochs and evaluate on the last 20% of total dataset. For each trial we repeat with 3 seeds and calculate the mean value as well as standard deviation of the corresponding metrics.

## 5.2 Incremental representation learning and clustering

Figure 4 displays the unsupervised clustering accuracy achieved by our proposed method on three datasets: (a) MNIST, (b) Fashion-MNIST, and (c) Reuters10k. We train the model on datasets with a fixed number of ground truth classes and gradually increase the class number in the subsequent trials. The bar plot represents the mean values of clustering accuracy along with the corresponding standard deviation. Our framework consistently achieves high clustering accuracy, with an average accuracy of 91% and 71% on MNIST and Fashion-MNIST datasets, respectively, and over 80% on Reuters10k dataset. Notably, our approach outperforms the baseline frameworks GMVAE and GMM that require prior specification of the number of clusters. In the case of larger feature sets than the number of pre-defined clusters, the clustering accuracy of these baseline models significantly declines due to its inherent limitation about unchangeable cluster number in prior space.

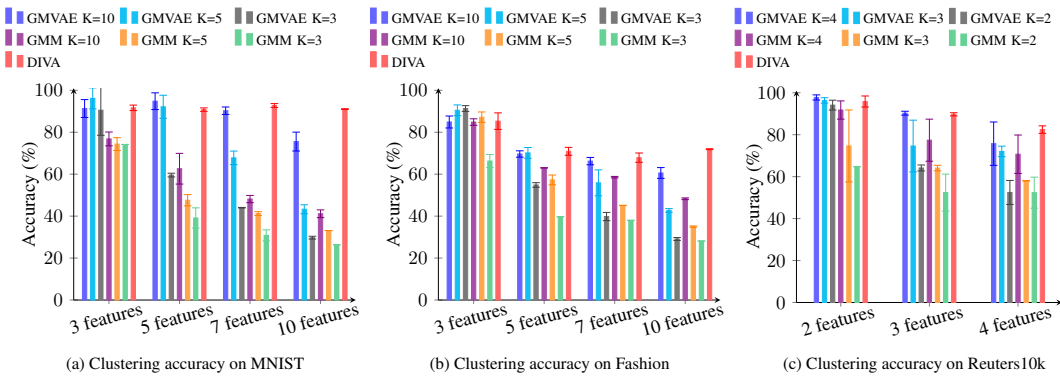


Figure 4: Unsupervised cluster accuracy for (a) MNIST, (b) Fashion-MNIST and (c) Reuters10k. We evaluate our framework and baselines on test dataset with incremental features, e.g. for MNIST the x-axis with “3 features” means the dataset only contains 3 different types of digit to be classified, which are “0, 1, 2” respectively.

To quantify the performance, Table 1 displays the accuracy statistics on the MNIST test set for our proposed framework DIVA and the baseline methods. The values in the table represent the mean percentage of three trials, with the standard deviation  $\sigma$  indicated in brackets. Our framework

consistently maintains high clustering accuracy on the MNIST dataset, even as the number of features gradually increases in each new trial. In contrast, the accuracy of other baseline methods declines significantly when the number of features exceeds their corresponding predefined cluster number. Please see our supplementary material Sec. A.3 for additional results on other datasets.

Table 1: Unsupervised clustering accuracy (%) on MNIST dataset

# features	DIVA	GMVAE K=10	GMVAE K=5	GMVAE K=3	GMM K=10	GMM K=5	GMM K=3
3 features	91.64[ $\pm 1.31$ ]	91.31[ $\pm 4.26$ ]	96.15[ $\pm 5.01$ ]	89.11[ $\pm 14.36$ ]	76.82[ $\pm 3.30$ ]	74.35[ $\pm 3.06$ ]	74.17[ $\pm 0.01$ ]
5 features	90.80[ $\pm 0.81$ ]	94.81[ $\pm 3.99$ ]	92.14[ $\pm 5.50$ ]	59.58[ $\pm 0.89$ ]	62.61[ $\pm 7.32$ ]	47.57[ $\pm 2.69$ ]	39.13[ $\pm 4.83$ ]
7 features	<b>92.76[<math>\pm 0.91</math>]</b>	90.27[ $\pm 1.78$ ]	67.79[ $\pm 3.23$ ]	44.02[ $\pm 0.13$ ]	48.15[ $\pm 1.73$ ]	41.23[ $\pm 0.90$ ]	30.84[ $\pm 2.62$ ]
10 features	<b>91.02[<math>\pm 0.18</math>]</b>	75.55[ $\pm 4.50$ ]	43.30[ $\pm 2.13$ ]	29.74[ $\pm 0.67$ ]	41.14[ $\pm 1.84$ ]	33.11[ $\pm 0.01$ ]	26.33[ $\pm 0.05$ ]

To assess the effectiveness of our framework in learning a latent representation suitable for clustering, we train a  $k$ -Nearest Neighbor (kNN) [34] classifier using the latent samplings generated by both our framework and the baselines. The kNN error rates with  $k = 3, 5, 10$  are recorded as averages of 3 trials, expressed in percentage. All datasets consist of full features. The results presented in Table 2 demonstrate that our framework achieves the lowest error rate across all three datasets.

Table 2: Test error-rate (%) for kNN on MNIST, Fashion-MNIST and Reuters10k

Frameworks	MNIST kNN error			Fashion kNN error				Reuters10k kNN error		
	k=3	k=5	k=10	k=3	k=5	k=10		k=3	k=5	k=10
GMVAE K=3	8.3	7.1	6.3	26.4	24.6	22.7	GMVAE K=2	8.1	8.0	7.5
GMVAE K=5	8.1	7.2	6.3	26.0	24.4	22.6	GMVAE K=3	8.3	7.9	7.3
GMVAE K=10	7.7	6.9	6.2	26.7	24.7	23.1	GMVAE K=4	7.9	7.3	7.3
SB-VAE	13.2	12.7	12.4	24.7	23.6	22.5		63.7	64.4	62.4
<b>DIVA</b>	<b>3.1</b>	<b>3.2</b>	<b>3.1</b>	<b>13.2</b>	<b>12.7</b>	<b>12.5</b>		<b>5.0</b>	<b>4.8</b>	<b>5.0</b>

Additionally, we present the t-SNE [35] projection of the learned latent space on the MNIST full dataset in Figure 5 for both DIVA and the baselines, to providing an intuitive observation. In the figures, each color represents one ground truth class, and the classes represented by the same color in different figures are also consistent. As shown in the figures, our DIVA is capable of learning a distinct and cluster-suitable representation, while other baseline methods, such as Stick-breaking VAE, fail to classify the data points from each other. The GMVAE model, with an appropriate number of clusters ( $K = 10$ ) (Fig. 5c), can learn a better clustering representation, but some clustering groups are still “stick” together. However, when the number of defined clusters is smaller than the number of features, the GMVAE model fails to learn a distinct latent representation (Fig. 5d, 5e).

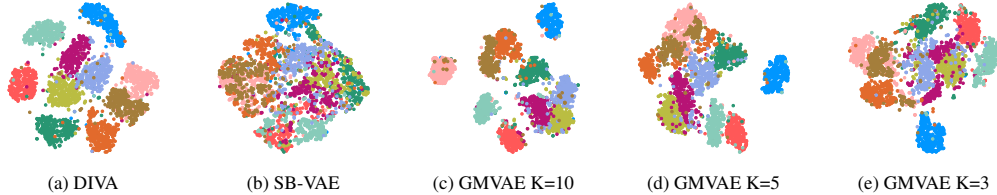


Figure 5: t-SNE latent representation on MNIST full dataset. Different colors indicate different true labels. It is clearly to see that our framework DIVA can learn a clustered latent representation with high distinction. Baselines like GMVAE with improper defined cluster number (Fig. 5d, 5e) are not able to learn a suitable clustering representation.

### 5.3 Dynamic adaptation

We evaluate the effectiveness of DIVA’s “birth” and “merge” moves during training via trials with the incremental features mode on the MNIST dataset. The models are initially trained with three digits, and we increase the number of digits at epochs 30, 60, and 90 to 5, 7, and 10, respectively. The test accuracy of all models (solid lines) and the number of cluster changes in DIVA (dashed line)



are depicted in Figure 6. As new features are added to the dataset, DIVA dynamically “births” new components to fit them, which may cause a temporary decrease in accuracy during the early stages of training as both the VAE and DP components are not yet converged. However, once training on the new subset converged, the accuracy return to the best possible performance. In contrast, baseline models such as GMVAEs lack this dynamic-adaptive capability. Once the number of features exceed the number of components, their test accuracy display a stepwise decline. Additional trial results please refer to the appendix Sec. A.3 and video visualization. The right plot in Figure 6 shows the latent space learned by DPMM, colored according to the clusters. It is observed that each ground truth class is learned by 2 or 3 sub-clusters, resulting in a total number of components greater than the number of ground truth classes, as demonstrated by the left plot. This is because DPMM captures not only the classes themselves but also the sub-features within each class. Moreover, after achieving convergence during training on the provided observations, the mapping between clusters and ground truth remains consistent and does not undergo shuffling.

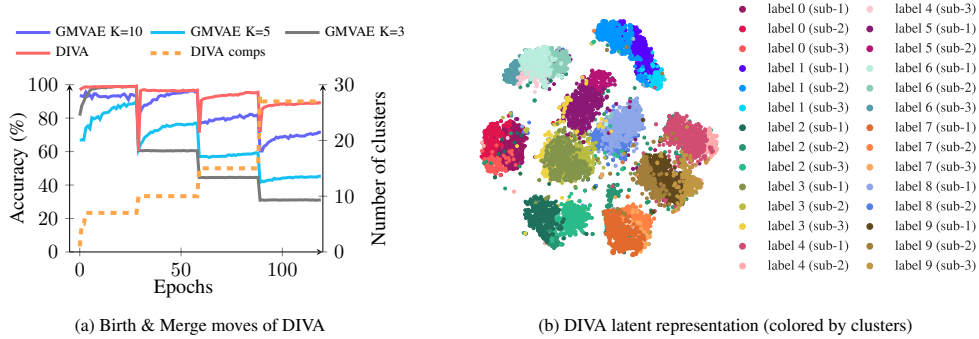


Figure 6: (a) “Birth” and “merge” moves of DIVA on MNIST. We introduce dynamic feature in training, where the model was initially trained on 3 digits, and the number of digits is increased to 5, 7, and 10 at epochs 30, 60, and 90. We record the test accuracy (solid lines) and the number of clusters for DIVA (dashed line). (b) t-SNE of DIVA on full MNIST, colored by clusters. Each true label is learned by 2 or 3 clusters, enabling the sub-features of individual digits to be captured.

To gain more insight into what individual sub-cluster has learned, we conducted image reconstructions using the components in the DPMM. Specifically, we sampled latent variables from each sub-cluster and then fed them to the decoder to rebuild images. The generated images from sub-clusters on MNIST (a)-(f) and Fashion-MNIST (g)-(l) are shown in Figure 7. The results demonstrate that each sub-cluster is capable of capturing distinct sub-features of the corresponding class. For instance, 3 sub-clusters that cluster the digit “0” in (a)-(c), have additionally learned different writing style of “0”. Similar conclusions can also be get from other examples. In summary, our proposed framework efficiently extracts informative sub-features from rough class labels. In particular, when dealing with unknown data features, our framework’s disentangled representation learning capability is highly beneficial in uncovering deep information from data samples.

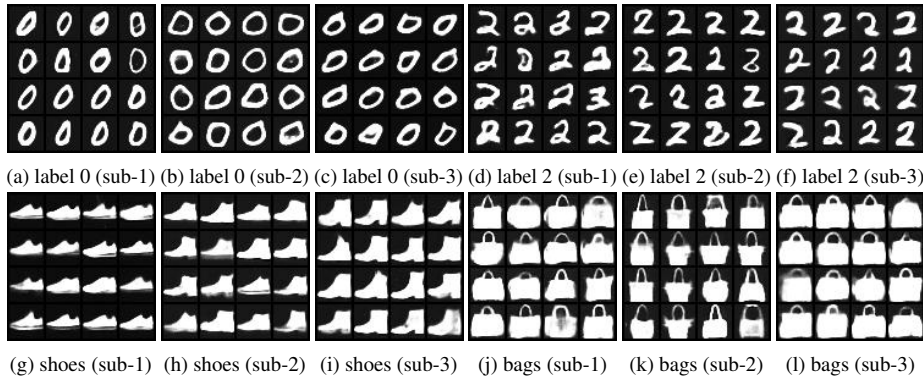


Figure 7: Reconstruction from DPMM clusters on MNIST (a)-(f) and Fashion-MNIST (g)-(l). Each class is learned by 2 or 3 sub-clusters, each cluster learns the sub-feature of individual class.

## 6 Conclusion

Our proposed framework, DIVA, utilizes the infinite clustering property of Bayesian non-parametric mixtures and combines it with the powerful latent representation learning ability of VAEs to overcome the challenge of clustering complex or dynamically changing data without prior knowledge of the feature number. The dynamic adaptation exhibited by DIVA on three datasets outperforms state-of-the-art baselines in handling data with incremental features. In addition, our framework excels in discovering finer-grained features and its adaptability to observed data suggests potential applications in domains like continuous learning. We encourage readers to explore further extensions and applications based on our framework.

## References

- [1] Zhou, S.; Xu, H.; Zheng, Z.; Chen, J.; Li, Z.; Bu, J.; Wu, J.; Wang, X.; Zhu, W.; Ester, M. A Comprehensive Survey on Deep Clustering: Taxonomy, Challenges, and Future Directions. 2022.
- [2] Ren, Y.; Pu, J.; Yang, Z.; Xu, J.; Li, G.; Pu, X.; Yu, P. S.; He, L. Deep Clustering: A Comprehensive Survey. 2022.
- [3] Aggarwal, C. C.; Zhai, C. A survey of text clustering algorithms. *Mining text data* **2012**, 77–128.
- [4] Yin, J.; Wang, J. A dirichlet multinomial mixture model-based approach for short text clustering. Proceedings of the 20th ACM SIGKDD international conference on Knowledge discovery and data mining. 2014; pp 233–242.
- [5] Kim, J.; Jeong, K.; Choi, H.; Seo, K. GAN-based anomaly detection in imbalance problems. Computer Vision–ECCV 2020 Workshops: Glasgow, UK, August 23–28, 2020, Proceedings, Part VI 16. 2020; pp 128–145.
- [6] Kingma, D. P.; Welling, M. Auto-Encoding Variational Bayes. 2022.
- [7] Reynolds, D. A., et al. Gaussian mixture models. *Encyclopedia of biometrics* **2009**, 741.
- [8] Nalisnick, E.; Smyth, P. Stick-breaking variational autoencoders. *arXiv preprint arXiv:1605.06197* **2016**,
- [9] Hughes, M. C.; Sudderth, E. Memoized online variational inference for Dirichlet process mixture models. *Advances in neural information processing systems* **2013**, 26.
- [10] Robins, A. Catastrophic forgetting, rehearsal and pseudorehearsal. *Connection Science* **1995**, 7, 123–146.
- [11] De Lange, M.; Aljundi, R.; Masana, M.; Parisot, S.; Jia, X.; Leonardis, A.; Slabaugh, G.; Tuytelaars, T. A continual learning survey: Defying forgetting in classification tasks. *IEEE transactions on pattern analysis and machine intelligence* **2021**, 44, 3366–3385.
- [12] Bing, Z.; Lerch, D.; Huang, K.; Knoll, A. Meta-Reinforcement Learning in Non-Stationary and Dynamic Environments. *IEEE Transactions on Pattern Analysis and Machine Intelligence* **2023**, 45, 3476–3491.
- [13] Wang, M.; Bing, Z.; Yao, X.; Wang, S.; Su, H.; Yang, C.; Huang, K.; Knoll, A. Meta-Reinforcement Learning Based on Self-Supervised Task Representation Learning. *arXiv preprint arXiv:2305.00286* **2023**,
- [14] Bing, Z.; Knak, L.; Cheng, L.; Morin, F. O.; Huang, K.; Knoll, A. Meta-Reinforcement Learning in Nonstationary and Nonparametric Environments. *IEEE Transactions on Neural Networks and Learning Systems* **2023**, 1–15.
- [15] Jin, X.; Han, J. K-Means Clustering. Encyclopedia of Machine Learning. Boston, MA, 2010; pp 563–564.
- [16] Li, Y.; Schofield, E.; Gönen, M. A tutorial on Dirichlet process mixture modeling. *Journal of mathematical psychology* **2019**, 91, 128–144.

- [17] Griffiths, T.; Jordan, M.; Tenenbaum, J.; Blei, D. Hierarchical Topic Models and the Nested Chinese Restaurant Process. *Advances in Neural Information Processing Systems*. 2003.
- [18] Qiang, J.; Li, Y.; Yuan, Y.; Wu, X. Short text clustering based on Pitman-Yor process mixture model. *Applied Intelligence* **2018**, *48*, 1802–1812.
- [19] Teh, Y.; Jordan, M.; Beal, M.; Blei, D. Sharing clusters among related groups: Hierarchical Dirichlet processes. *Advances in neural information processing systems* **2004**, *17*.
- [20] Xie, J.; Girshick, R.; Farhadi, A. Unsupervised Deep Embedding for Clustering Analysis. 2016.
- [21] Tian, K.; Zhou, S.; Guan, J. Deepcluster: A general clustering framework based on deep learning. *Machine Learning and Knowledge Discovery in Databases: European Conference, ECML PKDD 2017, Skopje, Macedonia, September 18–22, 2017, Proceedings, Part II* **2017**; pp 809–825.
- [22] Gansbeke, W. V.; Vandenhende, S.; Georgoulis, S.; Proesmans, M.; Gool, L. V. SCAN: Learning to Classify Images without Labels. 2020.
- [23] Jiang, Z.; Zheng, Y.; Tan, H.; Tang, B.; Zhou, H. Variational Deep Embedding: An Unsupervised and Generative Approach to Clustering. 2017.
- [24] Dilokthanakul, N.; Mediano, P. A.; Garnelo, M.; Lee, M. C.; Salimbeni, H.; Arulkumaran, K.; Shanahan, M. Deep unsupervised clustering with gaussian mixture variational autoencoders. *arXiv preprint arXiv:1611.02648* **2016**,
- [25] Yu, Y.; Zhou, W.-J. Mixture of GANs for Clustering. *IJCAI*. 2018; pp 3047–3053.
- [26] Radford, A.; Metz, L.; Chintala, S. Unsupervised Representation Learning with Deep Convolutional Generative Adversarial Networks. 2016.
- [27] Ntelemis, F.; Jin, Y.; Thomas, S. A. Image Clustering Using an Augmented Generative Adversarial Network and Information Maximization. *IEEE Transactions on Neural Networks and Learning Systems* **2022**, *33*, 7461–7474.
- [28] Ying, H.; Wang, H.; Shao, T.; Yang, Y.; Zhou, K. Unsupervised Image Generation with Infinite Generative Adversarial Networks. 2021.
- [29] Teh, Y. W. Dirichlet Process. *Encyclopedia of Machine Learning*. Boston, MA, 2010; pp 280–287.
- [30] Orbanz, P.; Teh, Y. W. Bayesian Nonparametric Models. *Encyclopedia of machine learning* **2010**, *1*.
- [31] Blei, D. M.; Jordan, M. I. Variational inference for Dirichlet process mixtures. 2006.
- [32] LeCun, Y.; Cortes, C.; Burgess, C. The MNIST Database of handwritten images. 2012.
- [33] Xiao, H.; Rasul, K.; Vollgraf, R. Fashion-mnist: a novel image dataset for benchmarking machine learning algorithms. *arXiv preprint arXiv:1708.07747* **2017**,
- [34] Kramer, O.; Kramer, O. K-nearest neighbors. *Dimensionality reduction with unsupervised nearest neighbors* **2013**, 13–23.
- [35] Cieslak, M. C.; Castelfranco, A. M.; Roncalli, V.; Lenz, P. H.; Hartline, D. K. t-Distributed Stochastic Neighbor Embedding (t-SNE): A tool for eco-physiological transcriptomic analysis. *Marine genomics* **2020**, *51*, 100723.
- [36] Pedregosa, F. et al. Scikit-learn: Machine Learning in Python. *Journal of Machine Learning Research* **2011**, *12*, 2825–2830.

## A Supplementary Material

### A.1 Variational inference of Dirichlet process mixture model

We draw generative graphic models for both GMM and DPMM in supplementary Figure 1 to provide an intuitive understanding about the generative process of DP mixture.

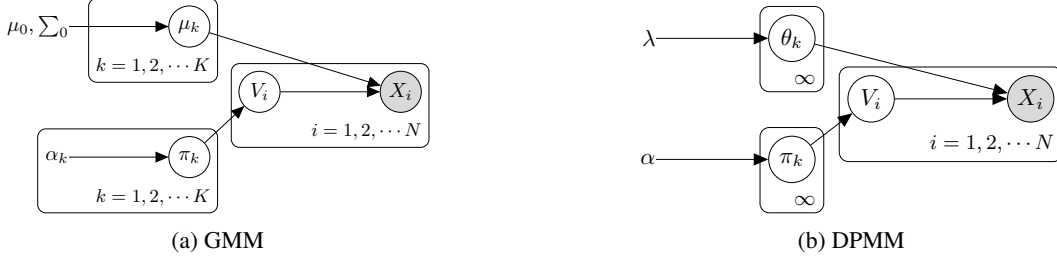


Figure 1: Generative graphic model of (a) the Gaussian mixture model and (b) the Dirichlet process mixture model. Compared with GMM that has fixed numbers of clusters, DPMM can model an infinite number of clusters.

Given a set of observations  $\mathbf{x} = \{x_1, \dots, x_N\}$ , recall that we can represent a Gaussian mixture model (GMM) as a generative model as follows:

$$\begin{aligned} \mu_i &\sim \mathcal{N}(\mu_0, \Sigma_0) \\ \pi_{1:K} &\sim \text{Dirichlet}(\alpha_{1:K}) \\ v_i &\sim \text{Cat}(\pi_{1:K}) \\ x_i | v_i &\sim \mathcal{N}(\mu_{v_i}, \Sigma) \end{aligned} \quad (1)$$

where each  $v_i$  represents a latent cluster for  $x_i$  and  $\pi$ 's are the mixing proportions. The Dirichlet process mixture model (DPMM) is an infinite mixture model from Bayes non-parametrics where the number of cluster components is decided by the data instead of being pre-specified. A set of observations  $\mathbf{x} = \{x_1, \dots, x_N\}$  is modeled by a set of latent parameters  $\boldsymbol{\theta} = \{\theta_1, \dots, \theta_N\}$ , where  $\theta_i$  is draw from  $G$ . Here  $x_i$  is assumed to have distribution  $F(\theta_i)$  parameterized by  $\theta_i$ . Then we have

$$\begin{aligned} G | \alpha, H &\sim \text{DP}(\alpha, H) \\ \theta_i | G &\sim G \\ x_i | \theta_i &\sim F(\theta_i) \end{aligned} \quad (2)$$

Meanwhile, the Dirichlet process can be alternatively represented using the stick-breaking process. Given  $\alpha$  and  $H$ , we express  $G | \alpha, H \sim \text{DP}(\alpha, H)$  as follows:

- Sample cluster parameters  $\theta_k^* | H \sim H$  from the base distribution  $H$ .
- Sample the corresponding mixture proportions  $\pi | \alpha \sim \text{GEM}(\alpha)$ .
- Multiply the cluster parameters and mixture proportions to obtain a random discrete probability measure from the Dirichlet process, denoted as  $G$ .
- Use categorical distribution with mixture proportion  $\pi$  to get the cluster assignment, and corresponding cluster parameters  $\theta_{v_i}^*$ .

The generative process is further explained in Section 3.2 and summarized below.

$$\begin{aligned} \theta_k^* | H &\sim H \\ \pi | \alpha &\sim \text{GEM}(\alpha) \\ v_i | \pi &\sim \text{Cat}(\pi) \\ x_i | v_i &\sim F(\theta_{v_i}^*) \end{aligned} \quad (3)$$

According to the generative process eq.(3), the joint probability of DPMM  $p(\mathbf{x}, \mathbf{v}, \boldsymbol{\theta}, \boldsymbol{\beta})$  is written as:

$$p(\mathbf{x}, \mathbf{v}, \boldsymbol{\theta}, \boldsymbol{\beta}) = \prod_{n=1}^N F(x_n | \theta_{v_n}) \text{Cat}(v_n | \boldsymbol{\pi}(\boldsymbol{\beta})) \prod_{k=1}^{\infty} \mathcal{B}(\beta_k | 1, \alpha) H(\theta_k | \lambda) \quad (4)$$

Since true posterior  $p(\mathbf{v}, \boldsymbol{\theta}, \boldsymbol{\beta}|\mathbf{x})$  is intractable, thus we aim to find best distribution that minimize the KL divergence, namely:

$$q^*(\mathbf{v}, \boldsymbol{\theta}, \boldsymbol{\beta}) = \arg \min_q \mathbb{KL}(q(\mathbf{v}, \boldsymbol{\theta}, \boldsymbol{\beta})||p(\mathbf{v}, \boldsymbol{\theta}, \boldsymbol{\beta}|\mathbf{x})) \quad (5)$$

$$\mathbb{KL}(q(\mathbf{v}, \boldsymbol{\theta}, \boldsymbol{\beta})||p(\mathbf{v}, \boldsymbol{\theta}, \boldsymbol{\beta}|\mathbf{x})) = \mathbb{E}[\log q(\mathbf{v}, \boldsymbol{\theta}, \boldsymbol{\beta})] - \mathbb{E}[\log p(\mathbf{x}, \mathbf{v}, \boldsymbol{\theta}, \boldsymbol{\beta})] + \log p(\mathbf{x})$$

Since  $\log p(\mathbf{x})$  is not depend on  $q$ , according to the variational inference theory, this is equivalent to maximize the ELBO of  $q$ , which is

$$\begin{aligned} \text{ELBO}(q) &= \mathbb{E}[\log p(\mathbf{x}, \mathbf{v}, \boldsymbol{\theta}, \boldsymbol{\beta})] - \mathbb{E}[\log q(\mathbf{v}, \boldsymbol{\theta}, \boldsymbol{\beta})] \\ &= \mathbb{E}[\log p(\mathbf{x}|\mathbf{v}, \boldsymbol{\theta}, \boldsymbol{\beta})] - \mathbb{KL}(q(\mathbf{v}, \boldsymbol{\theta}, \boldsymbol{\beta})||p(\mathbf{v}, \boldsymbol{\theta}, \boldsymbol{\beta})) \end{aligned} \quad (6)$$

To enable computation of  $q(\mathbf{v}, \boldsymbol{\theta}, \boldsymbol{\beta})$ , here we assume that  $q$  follows mean-field assumption, where each latent variable has its variational factor and is mutually independent of each other.

$$q(\mathbf{v}, \boldsymbol{\theta}, \boldsymbol{\beta}) = \prod_{n=1}^N q(v_n|\hat{r}_n) \prod_{k=1}^K q(\beta_k|\hat{\alpha}_{k1}, \hat{\alpha}_{k0}) q(\theta_k|\hat{\lambda}_k), \quad (7)$$

$$\begin{aligned} q_{v_n} &= \text{Cat}(v_n|\hat{r}_{n1:n_K}) \\ q_{\beta_k} &= \mathcal{B}(\beta_k|\hat{\alpha}_{k1}, \hat{\alpha}_{k0}) \\ q_{\theta_k} &= H(\theta_k|\hat{\lambda}_k) \end{aligned} \quad (8)$$

In order to distinguish the parameters of the variational factors  $q$  from those of the generative model  $p$ , we denote the former with hats. The categorical factor  $q_{v_n}$  is constrained to a maximum of  $K$  components to enable efficient computation. However, as the variational distribution is merely an approximation, the true posterior remains infinite. By increasing the value of  $K$ , the variational distribution can approach the infinite posterior through the optimization of the ELBO.

In addition, we consider a special case where both  $H$  and  $F$  in (4) belong to the exponential family:

$$p_H(\theta_k|\lambda_0) = \mathbb{E}[\lambda_0^T t_0(\theta_k) - a_0(\lambda_0)] \quad (9)$$

$$p(x_n|\theta_k) = \mathbb{E}[\theta_k^T t(x_n) - a(\theta_k)] \quad (10)$$

In this case, the ELBO can be expressed in terms of the expected mass  $N_k$  and the expected sufficient statistic  $s_k(x)$  of each component  $k$  [9]:

$$\begin{aligned} \text{ELBO}(q) &= \sum_{k=1}^K (\mathbb{E}_q[\theta_k]^T s_k(x) - \hat{N}_k[a(\theta_k)] + \hat{N}_k[\log \pi_k(\beta)]) - \sum_{n=1}^N \hat{r}_{nk} \log \hat{r}_{nk} \\ &\quad + \mathbb{E}_q[\log \frac{\mathcal{B}(\beta_k|1, \alpha)}{q(\beta_k|\hat{\alpha}_{k1}, \hat{\alpha}_{k0})}] + \mathbb{E}_q[\log \frac{H(\theta_k|\lambda)}{q(\theta_k|\hat{\lambda}_k)}] \end{aligned} \quad (11)$$

Each variational factor can be updated iteratively in a sequential manner. The first step involves updating the *local* variational parameters for the categorical factor  $q_{v_n}$  associated with each cluster assignment:

$$\tilde{r}_{nk} = \exp(\mathbb{E}_q[\log \pi_k(\beta)] + \mathbb{E}_q[\log p(x_n|\theta_k)]) \quad (12)$$

$$\hat{r}_{nk} = \frac{\tilde{r}_{nk}}{\sum_{l=1}^K \hat{r}_{nl}} \quad (13)$$

Subsequently, we proceed to update the *global* parameters in the stick-breaking proportions factor  $q_{\beta_k}$  and the base distribution factor  $q_{\theta_k}$ .

$$\begin{aligned} \hat{N}_k &= \sum_{n=1}^N \hat{r}_{nk}, & \alpha_{k1} &= \alpha_1 + \hat{N}_k, & \alpha_{k0} &= \alpha_0 + \sum_{l=k+1}^N \hat{N}_l \\ s_k(x) &= \sum_{n=1}^N \hat{r}_{nk} t(x_n), & \hat{\lambda}_k &= \lambda_0 + s_k(x). \end{aligned} \quad (14)$$

We employ this coordinate ascent method to iteratively optimize the local and global parameters with the objective of maximizing the ELBO [9].

## A.2 Implementation details

### A.2.1 VAE architectures

For image datasets, we use convolutional neural networks (Conv2d), as depicted in suppl. Figure 2. The output activation function of decoder is *tanh*, the reconstruction loss is MSE loss with mean reduction mode. Conversely, for text datasets, we adopt full-connection (FC) layers as Multi-layer-processing (MLP) module, where we directly use the linear output of decoder as reconstruction without activation node, the structure is shown in suppl. Figure 3.

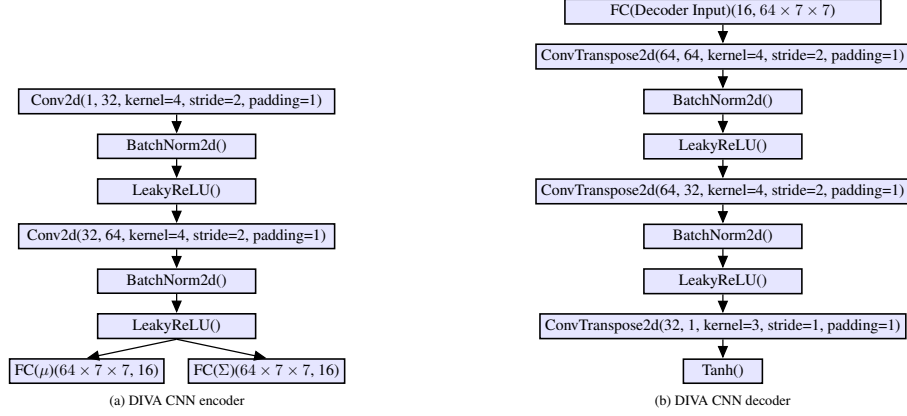


Figure 2: DIVA VAE Architecture for MNIST & Fashion-MNIST

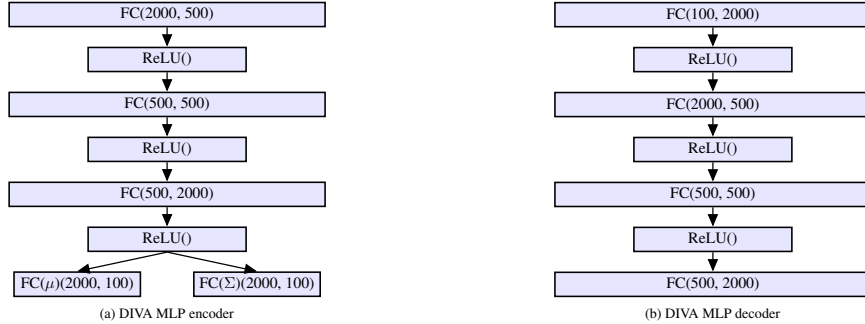


Figure 3: DIVA VAE Architecture for Reuters10k

### A.2.2 Hyper-parameters

In addition, we summarize the hyper-parameters that commonly in use for all trials in the following suppl. Table 1.

Table 1: Hyper-parameters of DIVA

Description	Variable name	Value
learning rate	LR	$1e-3$
learning rate decay	weight_decay	$1e-4$
train epoch(s)	max_epochs	100 (image), 15 (others)
batch size	batch_size	64
seed(s)	seed	1,2,3
KL divergence penalty factor	kld_weight	$1e-3$
optimizer	[-]	Adam
minimal number of atoms for new components	b_minNumAtomsForNewComp	80
minimal number of atoms for target components	b_minNumAtomsForTargetComp	100
minimal number of atoms for retain components	b_minNumAtomsForRetainComp	100
scale factor of observe model	sF	0.1

### A.2.3 Baseline frameworks setup

**SB-VAE.** We employ the VAE architecture of DIVA, incorporating a stick-breaking process to replace the Gaussian distribution in the latent space. The latent variable dimension and other hyperparameters remain consistent with DIVA, as detailed in suppl. Table 1.

**GMM.** We utilize the scikit-learn library [36] for GMM implementation. In all trials, we set the maximal iteration step to 100, while maintaining the covariance type of components as “diag”, consistent with DIVA.

**GMVAE.** We directly utilize the officially released source code of GMVAE [24]. The only modifications made are to the latent dimensions and the number of cluster components in the prior space. The training steps, batch size, and other hyperparameters remain consistent with DIVA. For further details, please refer to suppl. Table 1.

## A.3 Full experimental results of DIVA

### A.3.1 Metrics

In this paper, we employ the widely used metric of unsupervised clustering accuracy (ACC) as one of our evaluation criteria. The metric has been extensively utilized in prior studies and is widely accepted in the field [23, 24]. The formulation of the unsupervised clustering accuracy is presented below [23]:

$$ACC = \max_f \frac{\sum_{i=1}^N \mathbf{1}\{l_i = f(v_i)\}}{N} \quad (15)$$

where  $f$  is a mapping from the learned DPMM clusters to the true class labels  $l_i$ .  $N$  is the number of samples,  $v_i$  is corresponding cluster assignment.

We also incorporate the  $k$ -Nearest Neighbor (kNN) classification error rate as another evaluation metric. This involves training a kNN classifier using the learned latent variables. By utilizing this metric, we can assess the discriminative capabilities of the models within the latent space. Commonly chosen values for  $k$  include  $k = 1, 3, 5$  [20, 23]. The full test results are shown in Table 2 in the main page.

### A.3.2 Quantitative results of unsupervised clustering

Following tables display the unsupervised clustering accuracy on MNIST (suppl. Table 2), Fashion-MNIST (suppl. Table 3) and Reuters10k (suppl. Table 4). Each data point recorded as format “mean value (%) [ $\pm\sigma$ ]”. We run for each trial with seed=“1, 2, 3”, and record its mean value and corresponding standard deviation. To verify the model performance, we divide the datasets into train set and test set. For both MNIST and Fashion-MNIST datasets, we leverage torchvision implementation and use its default allocation ratio between train set and test set. For Reuters10k, we divide the whole dataset into 80% : 20%, where we use the 80% part as our train set, and 20% for test. In each trial we train frameworks on train dataset 100 epochs for MNIST and Fashion-MNIST, and 15 epochs for Reuters10k, and evaluate the performance on corresponding test dataset.

Table 2: Unsupervised clustering accuracy (%) on MNIST dataset

# features	DIVA	GMVAE K=10	GMVAE K=5	GMVAE K=3	GMM K=10	GMM K=5	GMM K=3
3 features	91.64[ $\pm 1.31$ ]	91.31[ $\pm 4.26$ ]	96.15[ $\pm 5.01$ ]	89.11[ $\pm 14.36$ ]	76.82[ $\pm 3.30$ ]	74.35[ $\pm 3.06$ ]	74.17[ $\pm 0.01$ ]
5 features	90.80[ $\pm 0.81$ ]	94.81[ $\pm 3.99$ ]	92.14[ $\pm 5.50$ ]	59.58[ $\pm 0.89$ ]	62.61[ $\pm 7.32$ ]	47.57[ $\pm 2.69$ ]	39.13[ $\pm 4.83$ ]
7 features	92.76[ $\pm 0.91$ ]	90.27[ $\pm 1.78$ ]	67.79[ $\pm 3.23$ ]	44.02[ $\pm 0.13$ ]	48.15[ $\pm 1.73$ ]	41.23[ $\pm 0.90$ ]	30.84[ $\pm 2.62$ ]
10 features	91.02[ $\pm 0.18$ ]	75.55[ $\pm 4.50$ ]	43.30[ $\pm 2.13$ ]	29.74[ $\pm 0.67$ ]	41.14[ $\pm 1.84$ ]	33.11[ $\pm 0.01$ ]	26.33[ $\pm 0.05$ ]

Table 3: Unsupervised clustering accuracy (%) on Fashion-MNIST dataset

# features	DIVA	GMVAE K=10	GMVAE K=5	GMVAE K=3	GMM K=10	GMM K=5	GMM K=3
3 features	85.29[ $\pm 3.95$ ]	84.89[ $\pm 2.85$ ]	90.48[ $\pm 2.56$ ]	91.31[ $\pm 1.37$ ]	84.86[ $\pm 1.55$ ]	87.18[ $\pm 2.49$ ]	66.28[ $\pm 3.12$ ]
5 features	70.91[ $\pm 1.89$ ]	69.63[ $\pm 1.52$ ]	70.15[ $\pm 2.58$ ]	54.86[ $\pm 1.09$ ]	63.01[ $\pm 0.01$ ]	57.28[ $\pm 2.33$ ]	39.70[ $\pm 0.01$ ]
7 features	67.89[ $\pm 2.21$ ]	66.24[ $\pm 1.75$ ]	55.89[ $\pm 6.17$ ]	39.81[ $\pm 1.95$ ]	58.58[ $\pm 0.36$ ]	45.11[ $\pm 0.01$ ]	37.99[ $\pm 0.01$ ]
10 features	71.91[ $\pm 0.21$ ]	60.58[ $\pm 2.57$ ]	42.73[ $\pm 0.86$ ]	29.11[ $\pm 0.68$ ]	48.28[ $\pm 0.42$ ]	35.00[ $\pm 0.32$ ]	28.14[ $\pm 0.01$ ]

Table 4: Unsupervised clustering accuracy (%) on Reuters10k dataset

# features	DIVA	GMVAE K=4	GMVAE K=3	GMVAE K=2	GMM K=4	GMM K=3	GMM K=2
2 features	95.83[±2.64]	97.77[±1.22]	96.35[±1.29]	94.11[±2.34]	91.77[±4.34]	74.65[±17.15]	64.75[±0.01]
3 features	89.71[±0.76]	90.62[±0.92]	74.60[±12.33]	64.14[±1.42]	77.39[±10.03]	64.09[±1.33]	52.39[±8.82]
4 features	82.44[±1.78]	75.73[±10.34]	72.03[±2.50]	52.47[±5.72]	70.70[±9.15]	58.02[±0.12]	52.35[±7.41]

### A.3.3 Dynamic adaptation

Suppl. Figure 4 shows the “birth & merge” moves of DIVA during training on MNIST dataset. We conduct 4 trials, where in the first 3 trials the model is trained under static case, which means the number of feature is unchanged during training and stable at 3, 5, 10 respectively. In the 4-th trial, the model is trained with dynamically increased features, where the feature number increases at epoch 30, 60, 90 from initial 3 to 5, 7, 10 respectively. It is worth noting that under static case, the DIVA births the appropriate number of clusters to fit the observation, once the training converges, the redundant clusters may merge to one to improve the ELBO of the inference. In dynamic changing feature case, the similar results could be acquired, the number of clusters may increase according to the increased feature number.

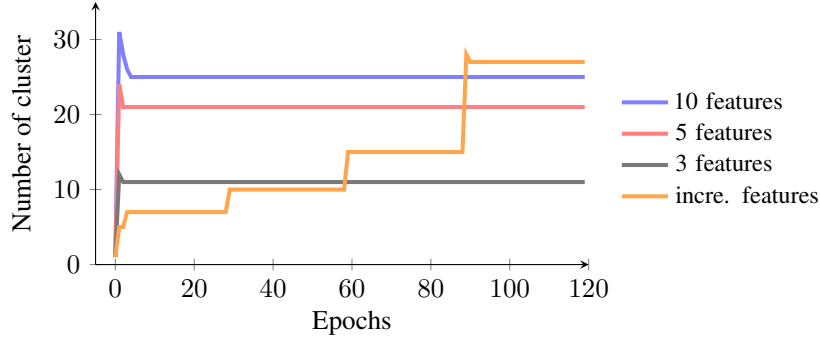


Figure 4: “Birth & Merge” moves of DIVA on MNIST. We conduct 4 trials, in which the number of features in the first 3 trials are static at 3, 5, 10 respectively. In the 4-th trial, the number of feature is initially at 3 and increases at epoch 30, 60, 90 to 5, 7, 10 respectively.

### A.4 Traceability of DPMM clustering learning

One remarkable characteristic of DIVA clustering is its traceability, wherein a cluster’s index position in the list and mapping to its corresponding ground truth label remain unchanged as long as the cluster does not undergo “birth” or “merge” moves. In our study, each individual cluster component in the DPMM is represented by a multivariate diagonal Gaussian distribution with parameter pairs  $\{\mu_k, \Sigma_k\}_{k=0:K}$ . The management of DPMM clustering is facilitated by manipulating the number, position and value of these parameters within a list object.

To provide a clear illustration, we present a simplified case in Suppl. Figure 5. Initially, DIVA is trained and converged on the MNIST dataset with only two ground truth labels, “0” and “1” (Suppl. Figure 5a), resulting in three clusters in the DPMM. Cluster 0 captures label “1”, while clusters 1 and 2 capture label “0”.

In the subsequent stage, we extend the dataset range to include three ground truth labels by adding the digits “2” to the dataloader (Supplementary Figure 5b). The original clusters in the DPMM fail to adequately represent the new features in the dataset. Consequently, during the fitting process, the DPMM generates five new clusters to capture the new features: three clusters learn digit “2”, and two clusters learn digit “0”. Subsequently, the DPMM attempts to merge redundant clusters to enhance the performance based on the ELBO. By merging the clusters 1 and 2 from the initial stage, which learned digit “0”, the original cluster 2 disappears, and the new merged cluster occupies index 1. As a result, all other newly formed clusters shift one position forward to positions 2...6, as shown in Suppl. Figure 5b.



However, the original cluster 0 from the initial stage does not participate in any birth or merge operations, thus maintaining its position in the management list and its mapping to ground truth label “1” unchanged.

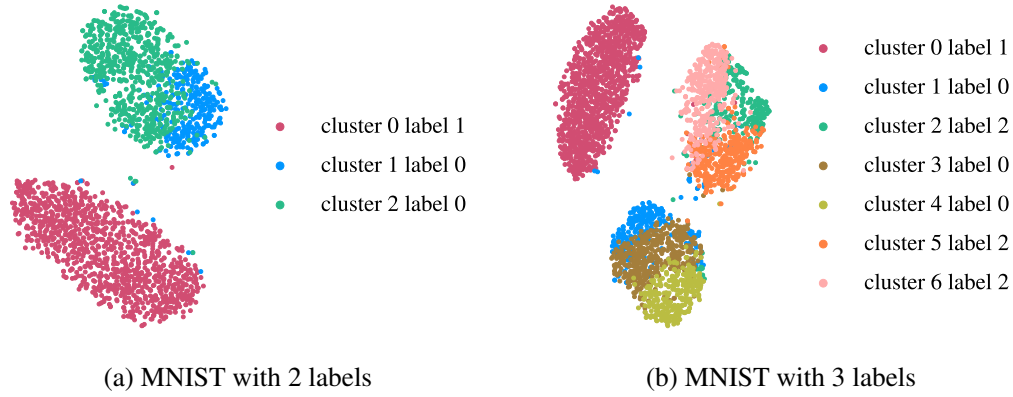


Figure 5: The t-SNE projection of MNIST with (a) 2 ground truth labels, (b) 3 ground truth labels, colored by clusters. Moving from subfigure (a) to (b), DIVA gains access to an additional label, namely “2”. During the fitting process, DIVA first generates 5 new clusters to accommodate the new observations. In the merging phase, the original clusters 1 and 2 in subfigure (a) merge into the new cluster 1 in subfigure (b). Simultaneously, all other newly formed clusters shift by one position, becoming clusters 2 to 6 in subfigure (b). Notably, cluster 0 remains unaffected by the birth and merge operations, maintaining its mapping and position intact within the cluster list.

### A.5 Shuffle the clusters may improve performance

In addition to the birth and merge proposals, we also introduce the “shuffle” moves as an alternative in the fitting process of DPM. After the birth and merge moves in each fitting lap, the “shuffle” move can be optionally activated, which rearranges the clusters based on the number of data points belonging to each active component and re-update the global parameters. This reordering places clusters with a larger number of data points at the forefront. This strategy can be beneficial for improving the ELBO by updating the global parameters and fast identifying potential more suitable candidates for birth and merge moves within a limited number of laps. Consequently, it may lead to an overall improvement in the clustering performance of DIVA. Supplementary Figure 6 illustrates an example of DIVA’s test accuracy on MNIST with and without the shuffle functionality. It is observed that incorporating shuffle moves leads to slightly improved performance compared to the setup without shuffle moves. Ultimately, the accuracy is improved by approximately 3% at the end of training.

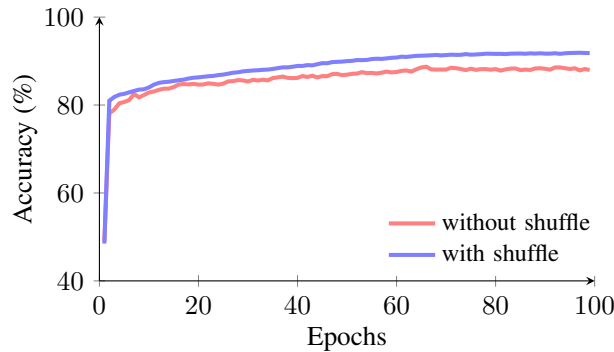


Figure 6: The test accuracy of DIVA trained on MNIST full dataset with additional “shuffle” moves (blue), and without “shuffle” moves (red).